The Gluon Contribution to the Sivers Effect COMPASS results



2016 J. Phys.: Conf. Ser. 678 012055

(http://iopscience.iop.org/1742-6596/678/1/012055)

# The Gluon Contribution to the Sivers Effect COMPASS results

**Krzysztof Kurek and Adam Szabelski on behalf of the COMPASS collaboration**
Adam Szabelski
National Centre for Nuclear Research
Hoza 69, 00-681 Warsaw
Poland

E-mail: adam.szabelski@cern.ch

**Abstract.** The Sivers effect describes the correlation between the spin of the nucleon and the orbital motion of partons. It can be measured via Semi-Inclusive Deep Inelastic Scattering of lepton on a transversely polarised proton and deuteron targets by determining the azimuthal asymmetry related to the modulation in the Sivers angle $\phi_{Siv}$. In the paper a method of obtaining the Sivers asymmetry for gluons is presented. It is based on the model of lepton nucleon interactions via three single-photon-exchange processes: photon-gluon fusion (PGF), QCD Compton (QCDC) and leading process (LP). A method of simultaneous extraction of the Sivers asymmetries of the three processes with the use of Monte Carlo (MC) and neural networks (NN) approach is presented. The method has been applied to COMPASS data taken with 160GeV/$c$ muon beam scattered off transversely polarised deuteron and transversely polarised proton target. For each target a data sample of events containing at least two hadrons with large transverse momentum has been selected. Finally the results for gluon Sivers asymmetry were obtained to be: $A_g^d = -0.14 \pm 0.15(stat.) \pm 0.06(syst.)$ at $\langle x_g \rangle = 0.13$ and $A_g^p = -0.26 \pm 0.09(stat.) \pm 0.08(syst.)$ at $\langle x_g \rangle = 0.15$.

## 1. Introduction

The transverse momentum dependent structure functions of the nucleon have been studied in semi-inclusive DIS on transversely polarised targets for many years. The strongest emphasis has been put on extracting Collins and Sivers asymmetry (Ref. [1] - deuteron target, Ref.[2] - proton target). In the COMPASS experiment kinematics these measurements are dominated by scattering of the muon on a quark.

To obtain the Sivers asymmetry for gluons from COMPASS data a model of unpolarised muon-nucleon scattering has been assumed. In this paper we use a LEPTO MC model (Ref. [3]) in which three single photon exchange processes: photon-gluon-fusion (PGF) $\gamma^* g \to q\bar{q}$, QCD Compton (QCDC) $\gamma^* q \to qg$ and the leading process (LP) $\gamma^* q \to q$ contibute. The above-mentioned analysis by COMPASS collaboration are dominated by the latter, the absorption of a virtual photon by a quark. To measure the Sivers effect for gluons (PGF Sivers asymmetry) a method of tagging PGF process is needed. The open charm meson production as in Ref. [4] gives a possibility to tag PGF process, however in the case of COMPASS data taken on transversely polarised targets the statistics is too small to extract the asymmetry from reconstructed charmed mesons. The other clean channel is the $J/\Psi$ production which is also not large in statistics.

Journal of Physics: Conference Series **678** (2016) 012055 doi:10.1088/1742-6596/678/1/012055

The remaining possibility is the observation of high-$p_T$ hadron pairs in the final state. The analysis presented in this paper is based on a method used for gluon polarisation $\Delta g/g$ determination, introduced in Ref.[5]. This analysis, described in detail in Section 3, uses Monte Carlo simulation and neural network (NN) approach. It enables to simultaneously extract asymmetries of the three contributing processes from a full set of events. The main difference between this analysis and the determination of $\Delta g/g$ is the modulation in the Sivers angle, $\phi_{Siv} \equiv \phi_{2h} - \phi_S$, where $\phi_{2h}$ is the azimuthal angle of the two high-$p_T$ hadrons observed in the final state and $\phi_S$ is the azimuthal angle of the spin direction of the nucleon. The angle $\phi_{2h}$ is measured on the hadron level and it is related to the gluon azimuthal angle $\phi_g$, unfortunately distorted by the fragmentation effects. Monte Carlo studies have shown that the strongest correlation between $\phi_g$ and $\phi_{2h}$ is when we define the latter as the azimuthal angle of the sum of the leading and next-to-leading hadron momenta. This correlation is further enhanced by the cuts on the transverse momenta of the two hadrons, $p_{T1} > 0.7\text{GeV}/c$, $p_{T2} > 0.4\text{GeV}/c$. The selection has been optimised taking into account the statistics of the sample and the $\phi_g, \phi_{2h}$ correlation. Moreover these cuts enhance the PGF fraction in the sample, Ref. [6].

## 2. Sivers asymmetry in two hadron production

With the above-mentioned selection the scattering of muon on nucleon with the production of at least two hadrons with large transverse momentum is studied:

$$\mu + N \to \mu' + 2h + X \tag{1}$$

The cross section for this reaction is described in details in Ref. [7] in terms of azimuthal angles $\phi_{2h}$ and $\phi_R$ corresponding to the vectors $\mathbf{P}_{2h} = \mathbf{P}_1 + \mathbf{P}_2$ and $\mathbf{R} = (\mathbf{P}_1 - \mathbf{P}_2)/2$ respectively. Where $\mathbf{P}_1$ and $\mathbf{P}_2$ are the leading and next-to-leading hadron momenta. In Ref. [8] and [9] have been shown that the Sivers modulation of the cross section, after integrating over $\phi_R$, is $\sin(\phi_{2h} - \phi_S)$. Here $\phi_S$ is the azimuthal angle of the spin of the nucleon.

Let us define the two hadron Sivers asymmetry by:

$$A_T^{2h}(\phi_{Siv}) = \frac{d^8\sigma^{\uparrow}(\phi_{Siv}) - d^8\sigma^{\downarrow}(\phi_{Siv})}{d^8\sigma^{\uparrow}(\phi_{Siv}) + d^8\sigma^{\downarrow}(\phi_{Siv})}. \tag{2}$$

Here $\phi_{Siv} = \phi_{2h} - \phi_S$. Then the number of events in a $\phi_{Siv}$ bin is given by:

$$N(\vec{x}, \phi_{Siv}) = \alpha(\vec{x}, \phi_{Siv}) \left(1 + f P_T A_T^{2h}(\phi_{Siv})\right), \tag{3}$$

where $\vec{x} = (x_{Bj}, Q^2, p_{T1}, p_{T2}, z_1, z_2)$, $f$ is the dilution factor and $P_T$ is the target polarisation. Here $\alpha = an\phi\sigma_0$, where $a$ is the total spectrometer acceptance, $n$ is the density of scattering centres, $\phi$ is the beam flux and $\sigma_0$ is the azimuthal independent part of the cross section. Throughout this paper only Sivers modulation will be taken into account:

$$N(\vec{x}, \phi_{Siv}) = \alpha(\vec{x}, \phi_{Siv}) \left(1 + f P_T A_{Siv}(\vec{x}) \sin\phi_{Siv}\right). \tag{4}$$

This can be done since azimuthal modulations given in Ref. [7] are orthogonal. The orthogonality has been confirmed during the systematics studies.

To obtain Sivers asymmetry for gluons from two hadron production in SIDIS it is necessary assume that the main contribution to the overall muon-nucleon scattering is due to three processes (Fig. 1) as presented in Ref. [3]. This model is successful in describing the unpolarised data. The leading process is in zero order QCD and is a dominating process. The other two, photon-gluon fusion and QCD Compton, are first order QCD processes and are suppressed. They can be enhanced, however, by the cut on $p_T$ of the produced hadrons. This is due to the

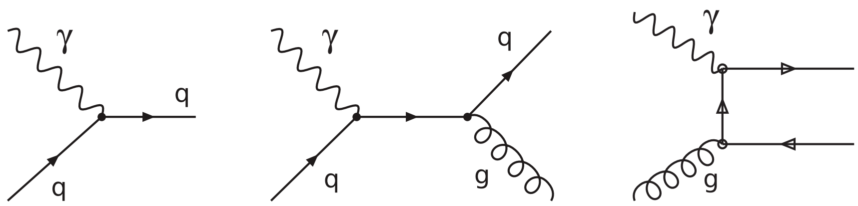


Figure 1: Feynman diagrams considered for $\gamma^* N$ scattering: a) Leading order process (LP), b) gluon radiation (QCD Compton scattering), c) photongluon fusion (PGF).

fact that hadrons in the leading process gain transverse momentum only from intrinsic parton transverse momentum and fragmentation while in the two other processes transverse momentum is also generated at the parton level as discussed in Ref. [6].
It has been checked on Monte Carlo data produced with the LEPTO generator that the fractions $R$ do not depend on $\phi_{Siv}$. Hence the Sivers asymmetry given in Eq. 4 can be decomposed into asymmetries of the sub-processes:

$$A_{Siv} = R_{PGF} A_{Siv}^{PGF} + R_{QCDC} A_{Siv}^{QCDC} + R_{LP} A_{Siv}^{LP}. \qquad (5)$$

## 3. The weighted method of asymmetry extraction

The method described in this section has been already applied to longitudinal data for $\Delta g/g$ extraction and featured in Ref [5]. For both, deuteron and proton, targets four target configurations can be introduced; in the case of two-cell target (deuteron): 1 - upstream, 2 - downstream, 3 - upstream′, 4 - downstream′, in the case of three-cell target (proton): 1 - (upstream+downstream), 2 - centre, 3 - (upstream′+downstream′), 4 - centre′. Here upstream′, centre′ and downstream′ denote the cells after the polarisation reversal and configuration 1 has the polarisation pointing upwards in the laboratory frame. Using Eq. 5 and introducing $\beta_t^j(\phi_{Siv}) = R_j f P_T \sin\phi_{Siv}$ one can rewrite Eq. 4:

$$\begin{aligned} N_t(\vec{x}, \phi_{Siv}) = \alpha_t(\vec{x}, \phi_{Siv}) \Big(1 &+ \beta_t^{PGF}(\phi_{Siv}) A_{Siv}^{PGF}(\vec{x}) \\ &+ \beta_t^{QCDC}(\phi_{Siv}) A_{Siv}^{QCDC}(\vec{x}) + \beta_t^{LP}(\phi_{Siv}) A_{Siv}^{LP}(\vec{x})\Big), \end{aligned} \qquad (6)$$

where the target configuration $t = 1, 2, 3, 4$. For each process a statistical weight is introduced chosen to be $\omega^j \equiv \beta^j / P_T$ which optimises the statistical and systematic error.

$$\begin{aligned} p_t^j \equiv \sum_{i=1}^{N_t} \omega_i^j = \tilde{\alpha}_t^j \Big(1 &+ \{\beta_t^G\}_{\omega^j} A_{PGF}^{\phi_{Sivers}}(\langle x_g \rangle) \\ &+ \{\beta_t^{QCDC}\}_{\omega^j} A_{QCDC}^{\phi_{Siv}}(\langle x_C \rangle) + \{\beta_t^{LP}\}_{\omega^j} A_{LP}^{\sin(\phi_{2h}-\phi_s)}(\langle x_{Bj} \rangle)) \end{aligned} \qquad (7)$$

where

$$\tilde{\alpha}_t = \int d\vec{x} d\phi_{Siv} \omega(\phi_{Siv}) \alpha_t(\vec{x}) \qquad (8)$$

is the integrated acceptance and

$$\{\beta\}_\omega = \frac{\int \beta(\phi_{Siv}) \omega(\phi_{Siv}) \alpha_t(\vec{x}) d\vec{x}}{\int \omega(\phi_{Siv}) \alpha_t(\vec{x}) d\vec{x}} \approx \frac{\sum_i \beta_i \omega_i}{\sum_i \omega_i}. \qquad (9)$$

The last approximation assumes that the raw asymmetries are small $\beta A_{Siv} \ll 1$.
In order to avoid approaching to zero for the integrated acceptance defined in Eq. 8 and

present in the denominator in Eq. 9 a binning in $\phi_{Siv}$ is introduced. Two bins $(\phi^1_{Siv}, \phi^2_{Siv}) = ([0,\pi],[\pi,2\pi])$ have been applied.
In addition it was assumed that $A_{Siv}$ is a linear function of $x$ what allows to write:

$$\left\{A_{Siv}(x)\right\}_{\beta\omega} = A_{Siv}(\langle x\rangle), \tag{10}$$

Here $x$ denotes the momentum fraction carried by parton in given sub-process and it is also assumed that $\{x_j\}_{\omega^k\beta^j_t} \approx \{x_j\}_{\omega^m\beta^j_b} \equiv \langle x_j\rangle \quad j,k,m = PGF, LP, QCDC$ and $t,b$ run over the target configurations $1,2,3,4$, which is true for both data samples.

The given set of 12 equations can be them reduced to three by writing:

$$r^j := \frac{p^j_1 p^j_4}{p^j_2 p^j_3}. \tag{11}$$

Using the assumption that the integrated acceptances ratio is the same before and after the polarisation reversal, $(\tilde{\alpha}^j_1\tilde{\alpha}^j_4)/(\tilde{\alpha}^j_2\tilde{\alpha}^j_3) = 1$ a solvable set of three equations for three unknowns (asymmetries) is obtained. Applying the afore mentioned binning in $\phi_{Siv}$ and setting a constraint for each asymmetry $A^j(\phi^1_{Siv}) = A^j(\phi^2_{Siv})$ doubles the set of equation which can then be solved by fitting procedure of $\chi^2$ minimisation:

$$\chi^2 = (\vec{R}-\vec{L})^T[prop(12,3)^T Cov(12,12) prop(12,3)]^{-1}(\vec{R}-\vec{L}). \tag{12}$$

Vectors $\vec{R}$ and $\vec{L}$ are defined by right hand side and left hand side of Eqs. 11. The former contains the asymmetries - parameters of the fit, while the latter is given by the measured values of $\omega^j_i$. The $Cov(12,12)$ matrix elements refer to correlations between pairs of $p^j_t$ defined in Eq. 7 and can be approximated by $Cov(p_x,p_y) \approx \sum_{N_t}\omega_x\omega_y$. The propagation matrix $prop(12,3)$ is given by $prop(m,n) = \partial r_n/\partial p_m$.

## 4. Monte Carlo optimisation and Neural Network training

This section is based on the previous analysis featured in Ref. [6] and Ref. [5]. In this analysis the NN package [10] has been used. The NN has been trained with a Monte Carlo sample with process identification. As an input vector a set of 6 kinematic variables have been chosen, $x_{Bj}, Q^2, p_{T1}, p_{T2}, p_{L1}, p_{L2}$. The latter are the longitudinal part of the hadron momenta. Good agreement of these 6 variables distributions between MC and data are required.

The comparison of the distribution of 6 variables used in NN training is shown in Fig. 2 for the deuteron target case. In case of proton 2010 data the comparison looks similar.
As it was said above the 6 kinematic variables has been used as an input vector for the NN training. The NN output has been parametrised by two values depending on the MC type sub-process. The artificial NN was not able to separate the three processes but for each of the process three probabilities $P_{NN}$ for PGF, LP and QCDC have been assigned. To validate the NN training a MC sample, statistically independent of the MC sample applied for the training, was used. In each bin of $P_{NN}$, assigned to every MC event by trained NN, true fraction based on process ID was calculated. The results of the comparison for NN trained with MC 2010 are presented in Fig. 3. The results for MC 2004 data are very similar and are omitted here for brevity. In conclusion, the agreement between $P_{NN}$ and $P_{MC}$ for all three processes is very good. As the agreement between MC and real data is also good it is assumed that the fractions in Eq. 5 can be assigned by the trained NN run on real data. In average $R^j = P^j_{NN}$.

## 5. Systematic uncertainties

The main source of systematic uncertainties in this analysis is the Monte Carlo dependence. To estimate this error different MC settings have been used in the process of Neural

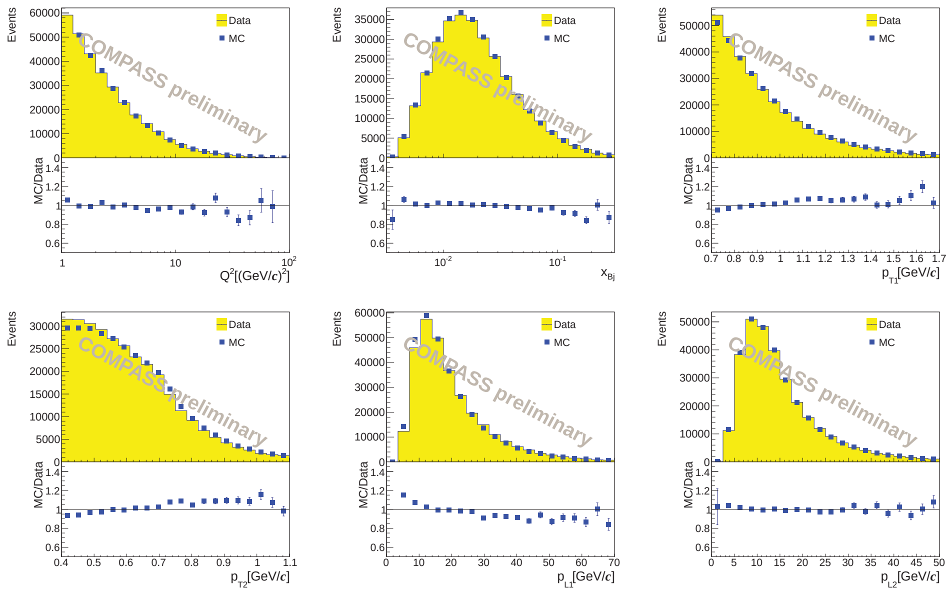


Figure 2: Kinematic variable distributions in MC and Data for high-$p_T$ samples normalised to the same number of events. Deuteron Data and MC 2004. Analogous plots have been obtained for Proton 2010 data

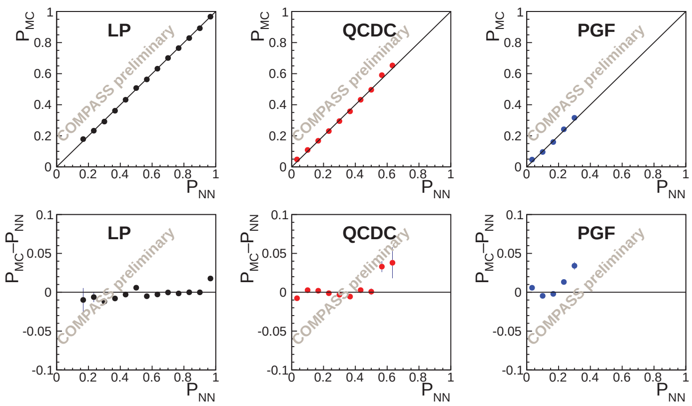


Figure 3: Neural network validation. Here $P_{NN}$ is the fraction of the process given by the NN and $P_{MC}$ is the true fraction of each process from MC in a given $P_{NN}$ bin.

Network training. Seven additional MC samples were prepared with different combinations of fragmentation parameters, tuning (default LEPTO and COMPASS high-$p_T$ tuning), Parton Shower on and off, different choices of the PDFs (MSTW08 or CTEQ5L, Ref.[11]) and $F_L$ from LEPTO and taken from the $R = \sigma_L/\sigma_T$, parametrisation of Ref. [12]. The choosen final Monte Carlo has the best agreement with the data presented in Fig. 2. All additional MCs use GEISHA instead of FLUKA secondary particle generator. For more details the reader is refered to Ref. [5]. Other estimated systematic uncertainties are listed in Table 1.

## 6. Results

The method presented in Sect. 3 with the use of trained NNs has been applied to the two data sets for deuteron and proton targets. The results are presented in Fig. 4. The gluon

| source | deuteron | | proton | |
|---|---|---|---|---|
| | value | % $\sigma_{stat}(=0.15)$ | value | % $\sigma_{stat}(=0.085)$ |
| Monte Carlo | 0.060 | 40% | 0.054 | 64% |
| False asymmetries | 0.016 | 11% | 0.032 | 38% |
| cut on hadron charges $q_1 \cdot q_2 = -1$ | 0.05 | 33% | 0.038 | 45% |
| radiative corrections | 0.018 | 12% | 0.018 | 21% |
| large $Q^2$ | - | - | 0.014 | 16% |
| $x_{Bj}$ binning | 0.07 | 47% | 0.011 | 13% |
| all asyms vs only Sivers | 0.003 | 2% | 0.005 | 6% |
| ML vs Weighted | 0.008 | 6% | 0.004 | 5% |
| target polarisation | 0.075 | 5% | 0.0043 | 5% |
| dilution factor | 0.003 | 2% | 0.0017 | 2% |
| total $\sqrt{\sum \sigma_i^2}$ | 0.13 | 88% | 0.078 | 92% |

Table 1: Systematic studies

Sivers two-hadron asymmetry for deuteron target, $A_g^d = -0.14 \pm 0.15(stat.) \pm 0.06(syst.)$ at $\langle x_g \rangle = 0.13$, is not in contradiction with the zero value while for proton target, $A_g^p = -0.26 \pm 0.09(stat.) \pm 0.08(syst.)$ at $\langle x_g \rangle = 0.15$, it is $3\sigma$ below zero. However, the obtained gluon Sivers asymmetries show compatibility between the two data samples which is consistent with the naive expectation that gluons are flavour-independent. The other two extracted asymmetries, for QCDC and LP, differ between the deuteron (isoscalar) target and the proton target.

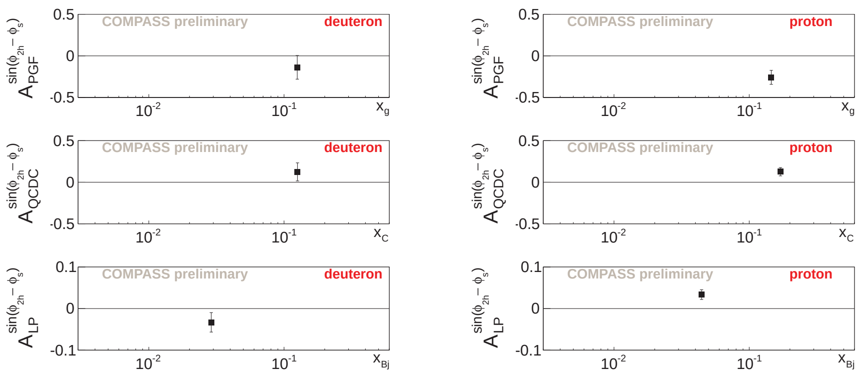


Figure 4: Sivers two-hadron asymmetry of the PGF $A_{PGF}^{sin(\phi_{2h}-\phi_S)}$, QCDC $A_{QCDC}^{sin(\phi_{2h}-\phi_S)}$ and LP $A_{LP}^{sin(\phi_{2h}-\phi_S)}$ for deuteron and proton targets.

## References

[1] Alekseev M *et al.* (COMPASS Collaboration) 2009 *Phys.Lett.* **B673** 127–135 (*Preprint* 0802.2160)
[2] Adolph C, Akhunzyanov R, Alexeev M, Alexeev G, Amoroso A *et al.* 2014 (*Preprint* 1408.4405)
[3] Ingelman G, Edin A and Rathsman J 1997 *Comput.Phys.Commun.* **101** 108–134 (*Preprint* hep-ph/9605286)
[4] Adolph C *et al.* (COMPASS Collaboration) 2013 *Phys.Rev.* **D87** 052018 (*Preprint* 1211.6849)
[5] Stolarski M (COMPASS) 2014 *PoS* **DIS2014** 211
[6] Adolph C *et al.* (COMPASS Collaboration) 2013 *Phys.Lett.* **B718** 922–930 (*Preprint* 1202.4064)
[7] Gliske S, Bacchetta A and Radici M 2014 *Phys.Rev.* **D90** 114027 (*Preprint* 1408.5721)
[8] Kotzinian A, Matevosyan H H and Thomas A W 2014 *Phys.Rev.Lett.* **113** 062003 (*Preprint* 1403.5562)
[9] Kotzinian A 2015 *Phys.Rev.* **D91** 054001 (*Preprint* 1408.6674)
[10] Sulej R Netmaker http://www.ire.pw.edu.pl/∼rsulej/NetMaker/
[11] Lai H *et al.* (CTEQ Collaboration) 2000 *Eur.Phys.J.* **C12** 375–392 (*Preprint* hep-ph/9903282)
[12] Abe K *et al.* (E143 Collaboration) 1999 *Phys.Lett.* **B452** 194–200 (*Preprint* hep-ex/9808028)